# pH Dependence of $^{15}N$ NMR Shifts and Coupling Constants in Aqueous Imidazole and 1-Methylimidazole. Comments on Estimation of Tautomeric Equilibrium Constants for Aqueous Histidine

**M. Alei, Jr.,*[1a] L. O. Morgan,[1b] W. E. Wageman,[1a] and T. W. Whaley[1a]**

*Contribution from The Los Alamos Scientific Laboratory, University of California, Los Alamos, New Mexico 87545, and the Department of Chemistry, The University of Texas, Austin, Texas 78712.* *Received September 14, 1979*

**Abstract:** $^{15}N$, $^{1}H$, and $^{13}C$ NMR spectra for [$^{15}N_2$]imidazole and [$^{15}N_2$]-1-methylimidazole in aqueous solution as functions of pH provide shift and coupling-constant information useful in characterizing the protonated and unprotonated forms of these compounds and as background for determining N binding to other species, such as metal ions. When combined with similar data for the imidazole-ring atoms in histidine, these data give more reliable estimates of tautomeric equilibrium constants for the amphionic and anionic forms of histidine than were possible from the histidine data alone.

The combination of high $^{15}N$ enrichment and pulsed Fourier-transform nuclear magnetic resonance (NMR) techniques provides sufficient sensitivity for the detailed investigation of nitrogen-containing compounds in solution at relatively low concentrations. Observations on imidazole and related compounds are of special interest because of the biological role of imidazole-ring nitrogens in many enzyme systems. In carbonic anhydrase, for example, the active site probably involves coordination of Zn(II) to the imidazole-ring nitrogen of histidine,[2a] while in the serine proteases the pH-dependent protonation–deprotonation of the imidazole ring of histidine probably plays an important role in the detailed mechanism of peptide-bond cleavage by these enzymes.[2b] In earlier publications[3] we have demonstrated the utility of $^{15}N$ NMR for studying complexation between imidazole and Zn(II) or Cd(II) in aqueous solution. In the present work we have investigated in detail the effects of the pH-dependent protonation–deprotonation on the $^{15}N$ NMR parameters of imidazole and 1-methylimidazole in aqueous solution.

The imidazole ring is a particularly important constituent of biological systems primarily because of the equilibrium shown in eq 1, with its unique p$K_a$ value near neutrality in

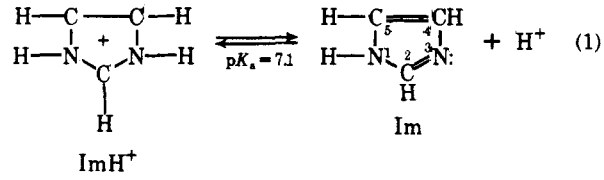


aqueous solution. This gives the imidazole ring the capability, in many biological fluids, of acting as a proton donor or acceptor and, perhaps most importantly, as a ligand which can coordinate metal ions. Characterization of the acidic and basic forms of imidazole and related compounds by virtue of their NMR properties has accordingly received a good deal of attention in recent years. Thus, Wasylishen and Tomlinson[4] have shown that the $^{13}C_2$–H and $^{13}C_4$–H nuclear spin–spin coupling constants both increase significantly in absolute magnitude when imidazole is converted to imidazolium ion in aqueous solution. More recently, these same authors have used long-range $^{13}C$–$^{1}H$ couplings in substituted imidazoles to draw inferences regarding imidazole tautomerism in L-histidine and related compounds.[5] Reynolds et al.[6,7] have used $^{13}C$ shift measurements on the imidazole-ring carbon atoms of L-histidine to derive similar information.

Prior $^{15}N$ NMR studies of systems containing the imidazole ring include a study of the $^{15}N$ shift as a function of pH for the imidazole nitrogens of histidine[8] and a more detailed study of $^{15}N$ shifts, coupling constants, and spin–lattice relaxation times for imidazole nitrogens of histidine as a function of pH.[9] Bachovchin and Roberts[2b] have recently reported $^{15}N$ shifts as a function of pH for the imidazole nitrogens of histidine in $\alpha$-lytic protease in aqueous solution. $^{15}N$ NMR studies of imidazoles in nonaqueous solution have also been reported.[10,11]

## Experimental Section

**Synthesis of [$^{15}N_2$]Imidazole.** The synthesis reported in an earlier publication[3] has been replaced by a modification which is not only easier to carry out, but also yields more than twice the amount of desired product. The procedure was as follows: 24 mL of a 40% aqueous solution of glyoxal (Aldrich, analyzed), 16 mL of a 37% aqueous solution of formaldehyde (Mallinckrodt, AR), and either 0.4 mol (21.8 g) of $^{15}NH_4Cl$ or 0.2 mol (26.4 g) of $(^{15}NH_4)_2SO_4$ were combined in a 500-mL Erlenmeyer flask with 24/40 ⅋ mouth. To the resulting slurry (the ammonium salt is not completely soluble at room temperature) was added dropwise, with continual stirring, a total of 23.5 mL of 50% aqueous NaOH. During the course of the addition (ca. 0.5 h) considerable heat was evolved (the reaction mixture rose in temperature to ca. 60 °C) and the reaction mixture proceeded from a light-yellow slurry to a light amber-colored solution, and finally to a dark reddish-brown slurry. The final reaction mixture was evaporated to dryness at 40–50 °C by attaching the Erlenmeyer flask to a rotary evaporator. The resulting brown solid was scraped off the walls of the Erlenmeyer flask and transferred to a vacuum sublimation apparatus where the crude [$^{15}N_2$]imidazole sublimed away readily at ca. 125 °C. A second vacuum sublimation of the crude material followed by one or two recrystallizations from $C_6H_6$ (product dissolved in ca. 10 mL of hot $C_6H_6$/g and cooled to ca. 10 °C for 1 or 2 h) yielded white, crystalline [$^{15}N_2$]imidazole melting at 89–90 °C. The yield was 45–50% (6–7 g) based upon the starting ammonium salt.

**[$^{15}N_2$]-1-Methylimidazole.** Reagents were obtained as follows: potassium hydride (Alfa Division, Ventron Corp., Danvers, Mass.), methyl *p*-toluenesulfonate (Eastman Organic Chemicals, Rochester, N.Y.), 1-methylimidazole (Aldrich Chemical Co., Milwaukee, Wis.). Gas chromatographic analyses were performed on a Varian Model 2100 instrument using an OV-225 column, He carrier gas, and temperature programming from 50 to 250 °C at 6 °C/min. Infrared spectra were recorded on a Perkin-Elmer Model 710 spectrophotometer.

Potassium hydride (16.5 g, 24.3% in mineral oil, 0.1 mol) was added to a 500-mL, three-neck flask, previously flushed with $N_2$ gas, and equipped with a mechanical stirrer, addition funnel, and condenser. The KH was washed three times with anhydrous petroleum ether (to remove mineral oil), and then suspended in 125 mL of anhydrous tetrahydrofuran (THF). A solution of [$^{15}N_2$]imidazole (7.02 g, 0.1 mol) in anhydrous THF (35 mL) was added over 30 min, and the mixture was stirred until $H_2$ evolution ceased. A solution of methyl

0002-7863/80/1502-2881$01.00/0 

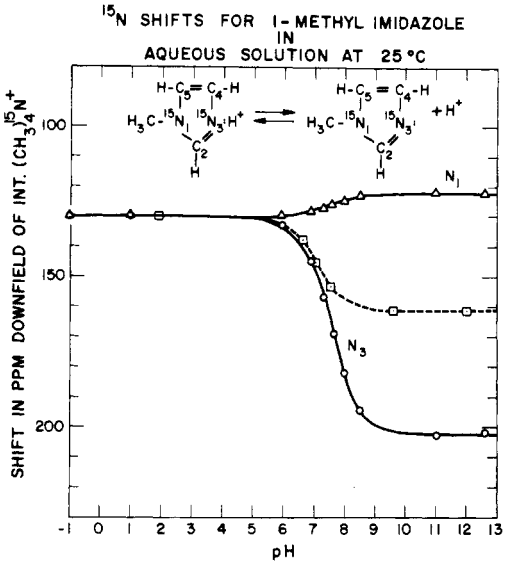


**Figure 1.** pH dependence of $^{15}$N NMR shifts for 1-methylimidazole in aqueous solution at 25 °C. (Dashed line through squares represents data for imidazole published previously.)[3]

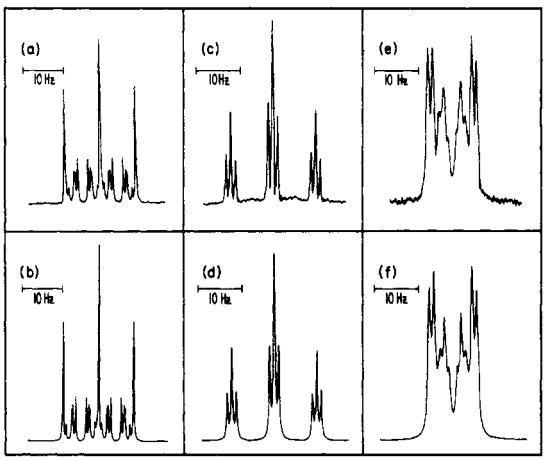


**Figure 2.** $^{15}$N and $^{1}$H NMR spectra of aqueous 1 M imidazole at 25 °C (pH 12): (a) 10.16-MHz $^{15}$N spectrum, 3965 transients, 19-$\mu$s pulse (30° tip angle), 20-s repetition rate, 100-Hz sweep width, 2048 points; (b), (d), (f) simulated $^{15}$N, $H_2$, and $H_{4,5}$ spectra, respectively; (c) 100-MHz $H_2$ spectrum, ambient temperature, 0.5-s frequency response, 500-s sweep time, 57-dB rf attenuation, $H_2O$ lock; (e) 100-MHz $H_{4,5}$ spectrum, as in (c).

*p*-toluenesulfonate (19.55 g, 0.105 mol) in THF (15 mL) was added over 5 min. The reaction mixture became quite warm, and vigorous stirring was necessary to dissipate the gel that formed. After the mixture was stirred for 1 h, water (50 mL) was added and the THF removed under reduced pressure. The aqueous residue was then placed in a continuous extractor and extracted with $CH_2Cl_2$ for 48 h. The $CH_2Cl_2$ solution was dried ($MgSO_4$) and the solvent removed on a steam bath. Distillation of the residue (80–90 °C, 19 mm) afforded [$^{15}N_2$]-1-methylimidazole (4.25 g, 50%) as a colorless liquid. The identity and purity of the product were confirmed, using IR and GC, by comparison with an authentic sample.

**Nuclear Magnetic Resonance Spectra.** The $^{15}$N spectra discussed in this work were taken at 25 °C on a Varian XL-100 spectrometer operating in FT mode at 10.16 MHz. Samples were ca. 2 mL of 1–2 M aqueous solutions of [$^{15}N_2$]imidazole or [$^{15}N_2$]-1-methylimidazole in 12-mm o.d. Pyrex sample tubes. $^{13}$C spectra were taken on the same instrument at 25.2 MHz or on a Varian CFT-20 spectrometer at 20 MHz. Proton spectra were taken on either a Varian HA-100 or EM-360 spectrometer in CW mode at ambient temperature (28–30 °C).

Accuracy of measured splittings is estimated to be ±0.2 Hz. Spectral simulations were done using NMRCAL,[12] which is applicable to two to six spin systems with spin ½ nuclei, on a Nicolet Instrument Corp. NIC 80 data processor. Transitions are calculated using perturbation theory[13,14] with estimated chemical shifts and coupling constants to obtain δ-function spectra (stick figures) upon which a single Lorentzian line shape is superimposed. Best values of input parameters were estimated by visual fitting of calculated and observed spectra for both $^{1}$H and $^{15}$N.

## Results and Discussion

The effect of pH variation on the relative proportions of acidic and basic forms of imidazole in aqueous solution leads to some interesting changes in the $^{15}$N spectrum. In the pH range 5–9, where significant amounts of both imidazole (Im) and imidazolium ion ($ImH^+$) are present, one observes a single $^{15}$N resonance of varying line width due to rapid $^{15}$N–H proton exchange between the two species. This exchange (probably involving $H_2O$ protons in the detailed mechanism) averages the 31.1-ppm shift in the average $^{15}$N resonance between the two species and leads to a single resonance with line width and resonant frequency dependent upon pH (ratio of $Im:ImH^+$). From an analysis of the $^{15}$N line widths in this pH region we infer[15] that the $ImH^+$–Im proton exchange rate (protons exchanged per second by an imidazole species) is given by $k[ImH^+][Im]$ with $k \simeq 1 \times 10^4$ s$^{-1}$ M$^{-1}$. Similar observations were made on the $^{15}N_3$ nitrogen of 1-methylimidazole.

At pH < 4 or >10, exchange makes a negligible contribution to the $^{15}$N line width since, in each case, only one species is present in significant amount. However, exchange of $^{15}$N–H protons with $H_2O$ is still rapid enough, in both cases, to preclude observation of any effects of coupling between $^{15}$N and a directly bonded proton. At high pH, this exchange also serves to make the nitrogens equivalent in the neutral species (Im), and one observes a single $^{15}$N resonance with well-resolved multiplet structure due to coupling with the C–H protons of the imidazole ring. Similarly at low pH one observes only the coupling between $^{15}$N and the C–H protons of imidazolium ion ($ImH^+$). However, if the acidity is increased to very high values (>6 M HCl), the exchange of solvent protons with $^{15}$N–H protons of $ImH^+$ is slowed sufficiently to permit observation of the directly bonded $^{15}$N–H coupling. The $^{15}N_3$ resonance of 1-methylimidazole displays similar behavior.

**$^{15}$N Shifts as a Function of pH.** $^{15}$N NMR shifts for $^{15}N_1$ and $^{15}N_3$ of 1-methylimidazole in aqueous solution as a function of pH are plotted in Figure 1. Also included in that figure are shift data for the averaged $^{15}$N resonance in imidazole as reported in an earlier publication.[3] The solid and dashed curves are drawn through the experimental points to aid in visual comparisons. They do, in fact, correspond closely to $pK_a = 7.1$ for imidazole and $pK_a = 7.2$ for 1-methylimidazole. Several important points should be made with regard to these data: (1) As expected, protonation of 1-methylimidazole at $^{15}N_3$ produces a large shift of the $^{15}N_3$ resonance (73.0 ± 0.2 ppm *upfield*) and a comparatively small shift at $^{15}N_1$ (8.0 ± 0.2 ppm *downfield*) relative to the unprotonated species. (2) At high pH, the averaged $^{15}$N resonance for imidazole appears at 161.5 ppm downfield of tetramethylammonium ion while the average for $^{15}N_1$ and $^{15}N_3$ of 1-methylimidazole is at 162.1 ppm on the same scale. (3) In 1-methylimidazolium ion (low pH), the $^{15}N_1$ and $^{15}N_3$ resonances essentially superpose at 129.5 ppm on the shift scale while the equivalent nitrogens in imidazolium ion are found at 129.7 ppm on the same scale. Observations (2) and (3) suggest strongly that replacement of a proton by a methyl group has a negligible effect on the $^{15}N_1$ chemical shift. This conclusion has also been drawn by Bachovchin and Roberts[2b] on the basis of similar observations.

**Coupling Constants.** The coupling constants derived in this work are summarized in Table I and some representative experimental and simulated $^{15}$N and $^{1}$H spectra are shown in Figures 2–4 to demonstrate typical spectral resolution and

**Table I.** Coupling Constants among $^{1}H$, $^{13}C$, and $^{15}N$ for Neutral, Cationic, and Anionic Species of Imidazole, 1-Methylimidazole, and Histidine[9] in Aqueous Solution at 25 °C

| | coupling constants, Hz | | | | | |
|---|---|---|---|---|---|---|
| | Im[a] | $ImH^{+}$ [b] | 1-MeIm | 1-$MeImH^{+}$ | $His^{-}$ | $His^{+(2+)}$ |
| $^{1}J_{C_2N_1}$ | −6.9 | −16.2 | −12.2 | −16.7 | −6.4 | −16.1 |
| $^{1}J_{C_2N_3}$ | | | −1.9 | −16.7 | −6.9 | −16.0 |
| $^{1}J_{C_5N_1}$ | −5.9 | −10.6 | −13.4 | −11.4 | −7.3 | −11.6 |
| $^{1}J_{C_4N_3}$ | | | +0.9 | −10.7 | −4.7 | −9.9 |
| $^{1}J_{CMeN_1}$ | | | −10.6 | −10.1 | | |
| $^{2}J_{C_4N_1}$ | ±0.9 | <0.5 | −4.8 | −0.9 | | |
| $^{2}J_{C_5N_3}$ | | | <0.5 | <0.5 | | |
| $^{2}J_{N_3N_1}$ | ±1.1 | | ±1.1 | ±1.7 | ±0.9 | ±0.9 |
| $^{1}J_{N_3H_3}$ | | −100.0 | | −101.0 | | |
| $^{2}J_{N_1H_2}$ | −9.6 | −5.5 | −7.6 | −5.0 | −8.8 | −4.6 |
| $^{2}J_{N_3H_2}$ | | | −10.8 | −5.4 | −9.6 | −6.1 |
| $^{2}J_{N_1H_5}$ | −7.2 | −4.0 to −4.6 | −5.5 | −4.4 to −5.2 | −6.6 | −4.8 |
| $^{2}J_{N_3H_4}$ | | | −9.0 | | | |
| $^{2}J_{N_1HMe}$ | | | −1.6 | −1.9 | | |
| $^{3}J_{N_1H_4}$ | −2.5 | −4.0 to −4.6 | −3.5 | −3.8 to −4.6 | −2.2 | −3.0 |
| $^{3}J_{N_3H_5}$ | | | −1.7 | | | |
| $^{3}J_{H_4H_5}$ | +1.4 | | | | | |
| $^{3}J_{H_2H_4}$ | +1.0 | +1.3 | +1.2 | +1.5 | | |
| $^{3}J_{H_2H_5}$ | | | +1.4 | +1.5 | | |

[a] Rapid proton exchange between $N_1$ and $N_3$ renders $N_1$ and $N_3$, $C_4$ and $C_5$, and $H_4$ and $H_5$ isochronous; only average coupling constants are experimentally observed. [b] The symmetry of the $ImH^{+}$ ion makes $N_1$ and $N_3$, $C_4$ and $C_5$, and $H_4$ and $H_5$ each an equivalent pair of nuclei.

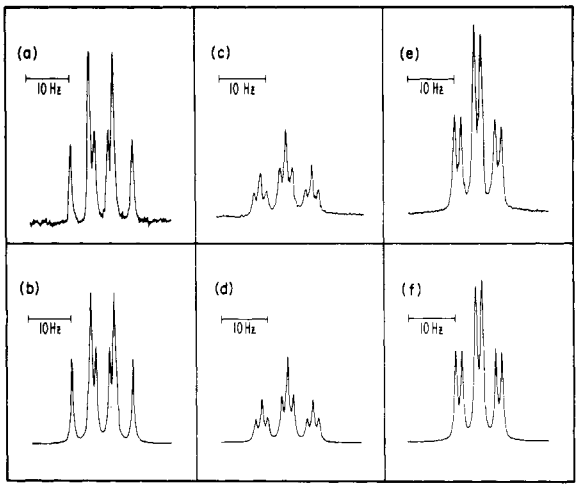


**Figure 3.** $^{15}N$ and $^{1}H$ NMR spectra of aqueous 1 M imidazolium ion (pH 4.0) at 25 °C: (a) 10.16-MHz $^{15}N$ spectrum, 70 transients, 50-μs pulse, 64-s repetition rate, 100-Hz sweep width, 1024 points; (b), (d), (f) simulated $^{15}N$, $H_2$, and $H_{4,5}$ spectra, respectively; (c) 100-MHz $H_2$ spectrum, as in Figure 2; (e) 100-MHz $H_{4,5}$ spectrum, as in Figure 2.

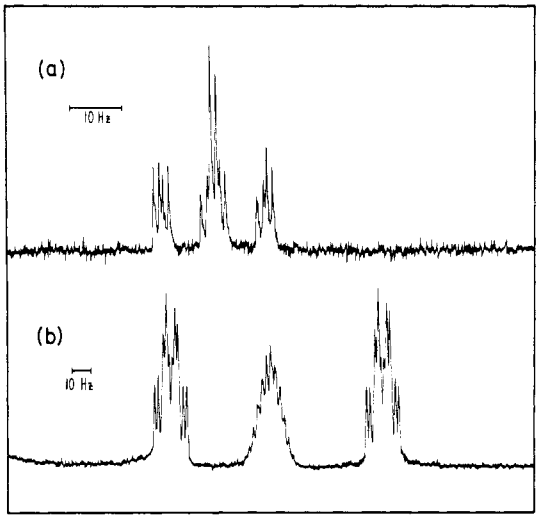


**Figure 4.** 10.16-MHz $^{15}N$ spectra for aqueous 1-methylimidazole at 25 °C: (a) $^{15}N_3$ spectrum for a 2 M solution (pH 12.7), 315 transients, 20-μs pulse, 20-s repetition rate, 100-Hz sweep width, 2048 points; (b) $^{15}N_1$ and $^{15}N_3$ (101-Hz doublet) peaks for 1.7 M 1-methylimidazolium ion in 8.5 M HCl.

quality of agreement between experimental and simulated spectra. To obtain optimal spectral resolution at high pH, it was usually necessary to treat the solutions with $H_2S$ to precipitate traces of paramagnetic impurities. This caused a drop in pH which was restored to near its initial value by flushing out dissolved $H_2S$ (with argon) and adding a small amount of NaOH solution. The $^{13}C^{15}N$ couplings, derived from natural-abundance $^{13}C$ spectra of the $^{15}N$-labeled materials, produced simple, first-order $^{13}C$ spectra from which the coupling constants could be derived by inspection.

To ensure proper assignment of the $C_4$ and $C_5$ resonances and to test for possible changes in sign of $^{13}C^{15}N$ coupling constants between 1-MeIm and 1-$MeImH^{+}$ we have recorded normal-abundance $^{13}C$ spectra for mixtures of 1-MeIm and 1-$MeImH^{+}$ covering the pH range from ~11 (100% 1-MeIm) to ~4 (100% 1-$MeImH^{+}$). Owing to rapid proton exchange between the two species, we anticipated that the shifts and couplings in a given mixture would be linearly weighted averages between the corresponding values for the acidic and basic forms. Furthermore, if a given coupling constant changes sign between the two forms, a plot of the magnitude of the coupling vs. mol % of one of the species should go through zero on the coupling-constant scale. Figures 5–7 summarize the observed $^{13}C$ shifts and $^{13}C^{15}N$ coupling constants as a function of mole fraction 1-$MeImH^{+}$. As anticipated, a plot of any of the NMR parameters vs. mole fraction 1-$MeImH^{+}$ is linear within experimental uncertainty. An interesting result is the crossover of the $C_4$ and $C_5$ resonance positions, $C_4$ being *downfield* of $C_5$ in 1-MeIm and *upfield* of $C_5$ in 1-$MeImH^{+}$. The observed chemical shifts and changes on protonation are quite consistent with those reported by Reynolds et al.[6] for imidazole, histidine, and various histidine derivatives. From their Figure 2, the protonation shifts for $C_2$, $C_4$, and $C_5$ in 1-methylhistidine are −3.4, −7.1, and +2.3 ppm, respectively, while the corresponding values for 1-MeIm are −2.9, −7.5, and +2.1 ppm. In Im the protonation changes are −2.4 ppm

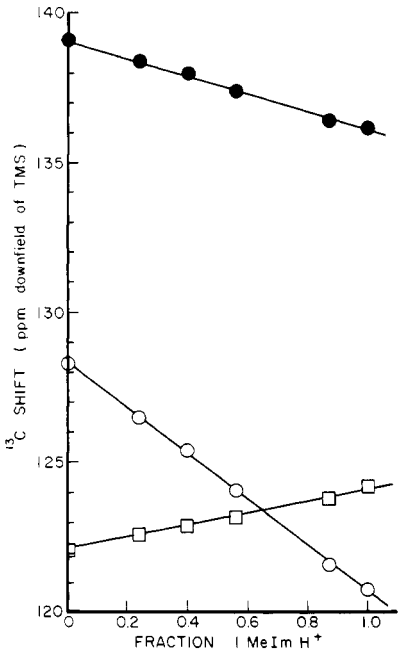


**Figure 5.** $^{13}$C shifts for aqueous mixtures of 1-MeIm and 1-MeImH$^+$ at 25 °C; $C_2$ = ●; $C_4$ = ○; $C_5$ = □.

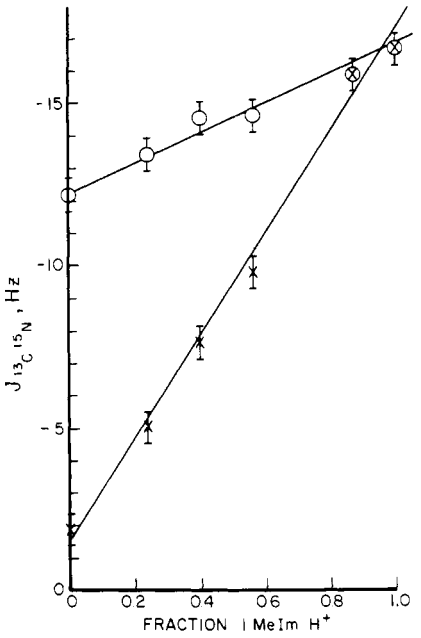


**Figure 6.** $^{13}C^{15}N$ coupling constants for aqueous mixtures of 1-MeIm and 1-MeImH$^+$ at 25 °C: $C_2$-$N_1$ = ○; $C_2$-$N_3$ = X.

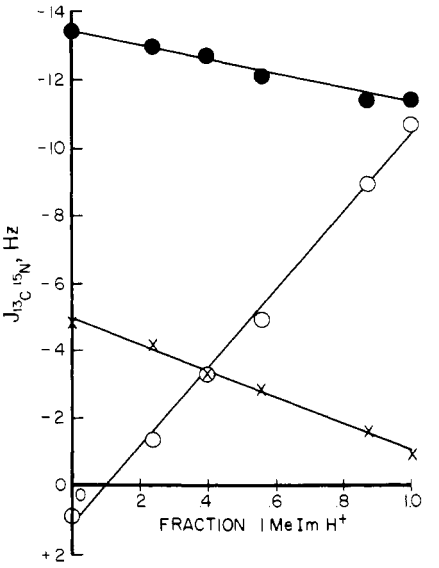


**Figure 7.** $^{13}C^{15}N$ coupling constants for aqueous mixtures of 1-MeIm and 1-MeImH$^+$ at 25 °C: $C_5$-$N_1$ = ●; $C_4$-$N_3$ = ○; $C_4$-$N_1$ = X.

for $C_2$ and −2.7 ppm for $C_{4,5}$; the average for $C_4$ and $C_5$ in 1-MeIm is −2.7 ppm. These results suggest that substitution of a methyl group for a proton at $N_1$ produces very small changes (if any) in the $^{13}$C shifts at $C_2$, $C_4$, and $C_5$.

With regard to the coupling-constant data, there is no evidence for a change in sign except for the $C_4N_3$ coupling where the plot of coupling constant vs. mol % 1-MeImH$^+$ is a much better straight line if the value of 0.9 is given a sign opposite to that for the other values. The $C_4$ multiplet is a doublet of doublets at both high and low pH limits, but is observed as a triplet where 1-methylimidazole is 40% protonated, so that the $C_4N_3$ and $C_4N_1$ coupling constants are apparently equal at that point (cf. Figure 7). Although the sign of $J_{C_4N_1}$ was not determined directly, it may be inferred, on the basis of calculated values (see below) for which relative values are expected to be more reliable than individual values, that the change on protonation is positive. That leads to negative values of $J_{C_4N_1}$ for both 1-MeIm and 1-MeImH$^+$.

To test for the possibility that the coupling constants might show a significant concentration dependence, we measured the $^{13}C^{15}N$ and $^{15}N^1H$ couplings in a 0.2 M solution of imidazole at high pH. The values were indistinguishable from those measured for 1 M solutions under the same conditions.

The coupling constants determined in this work are absolute values only. Following the practice of Blomberg et al.[9] we have assigned positive and negative values on the basis of experimental determinations for similar systems (see their discussion of the N–H constants and citations therein) and the theoretical outline of Schulman and Venanzi,[16] whenever possible. The latter authors have shown that a self-consistent-field calculation of the Blizzard-Santry[17] type yields $^{13}C^{15}N$ couplings which agree well with experimental values for a number of compounds. We have applied this calculational technique to imidazole and 1-methylimidazole in their basic and acidic forms using the same assumptions as those of ref 16. The results are summarized in Table II. The agreement between magnitudes of calculated and experimental values is very good for the large $^1J$ couplings involving $N_1$. In such cases it seems reasonable to conclude that the sign of the coupling constant is that given by the theoretical calculation. In other cases where the coupling magnitudes are small or there is poor agreement between the calculated and experimental magnitudes, any decision with regard to sign is less certain. It is interesting to note that, while calculated and observed values for 1-methylimidazole are in good agreement for $^1J_{C_2N_1}$, they are in poor agreement for $^1J_{C_2N_3}$. To explore the possibility that neglect of H bonding between $N_3$ and $H_2O$ molecules in the calculational model might be responsible for this discrepancy we (1) repeated the calculations assuming reasonable H-bonding models and (2) measured the CN coupling constants for 1-methylimidazole in $CH_2Cl_2$ and in $CHCl_3$. The results of the calculations showed that neglect of H bonding has little effect on the calculated couplings. The experimental measurements in the nonaqueous solvents (where H bonding between $N_3$ and solvent molecules is expected to be much weaker than in $H_2O$) are summarized in Table III and also suggest that the CN coupling constants are not very sensitive to whether or not $N_3$ is involved in H bonding. Thus, the discrepancy between calculated and experimental values for $^1J_{C_2N_3}$ remains unresolved.

Calculations on 4- or 5-methylimidazole showed that the

**Table II.** Comparison of Calculated and Experimental Values for $J_{^{13}C^{15}N}$ in $^{15}N$-Labeled Compounds (Hz)[a]

| molecule | bond | $J_{XN}^{FC}$ | $J_{XN}^{O}$ | $J_{XN}^{D}$ | $J_{XN}$ (total) | $J_{XN}$ (obsd) |
|---|---|---|---|---|---|---|
| imidazole[b] | $C_2N_1$ | −12.72 | +0.90 | −0.03 | −11.9 | −6.9 |
| | $C_2N_3$ | +6.50 | +1.77 | −0.44 | +7.8 | |
| | $C_5N_1$ | −14.57 | +0.77 | 0.00 | −13.8 | −5.9 |
| | $C_4N_3$ | +1.32 | +1.16 | −0.19 | +2.3 | |
| | $C_4N_1$ | −0.23 | −0.15 | −0.11 | −0.5 | ±0.9 |
| | $C_5N_3$ | +2.39 | −0.05 | +0.19 | +2.5 | |
| imidazolium ion[c] | $C_2N_1$ | −16.66 | +1.29 | −0.15 | −15.5 | −16.2 |
| | $C_2N_3$ | −16.66 | +1.29 | −0.15 | −15.5 | |
| | $C_5N_1$ | −11.28 | +0.76 | −0.04 | −10.6 | −10.6 |
| | $C_4N_3$ | −11.28 | +0.76 | −0.04 | −10.6 | |
| | $C_4N_1$ | +2.62 | −0.09 | +0.02 | +2.5 | <±1.0 |
| | $C_5N_3$ | +2.62 | −0.09 | +0.02 | +2.5 | |
| 1-methylimidazole[d] | $C_2N_1$ | −12.70 | +0.97 | −0.03 | −11.8 | −12.2 |
| | $C_2N_3$ | +5.93 | +1.80 | −0.04 | +7.3 | −1.9[e] |
| | $C_5N_1$ | −14.50 | +0.79 | 0.00 | −13.7 | −13.4 |
| | $C_4N_3$ | +1.44 | +1.16 | −0.19 | +2.4 | +0.9[e] |
| | $C_{Me}N_1$ | −10.35 | +0.21 | −0.13 | −10.3 | −10.6 |
| | $C_4N_1$ | −0.03 | −0.11 | −0.10 | −0.2 | −4.8[f] |
| | $C_5N_3$ | +2.44 | −0.06 | +0.19 | +2.6 | <1 |
| 1-methylimidazolium ion[g] | $C_2N_1$ | −16.24 | +1.37 | −0.20 | −15.1 | −16.7 |
| | $C_2N_3$ | −15.93 | +1.25 | −0.12 | −14.8 | −16.7 |
| | $C_5N_1$ | −11.58 | +0.80 | −0.06 | −10.8 | −11.4 |
| | $C_4N_3$ | −11.78 | +0.78 | −0.05 | −11.1 | −10.7 |
| | $C_{Me}N_1$ | −9.87 | +0.14 | −0.12 | −9.9 | −10.1 |
| | $C_4N_1$ | +2.81 | −0.07 | +0.04 | +2.8 | −1.0[f] |
| | $C_5N_3$ | +2.53 | −0.09 | +0.01 | +2.5 | <±1.0 |

[a] Parameters were $S_C^2(0)S_N^2(0) = 13.79a_0^{-3}$ and $\langle r^{-3}\rangle_C\langle r^{-3}\rangle_N = 1.77a_0^{-3}$, from J. M. Schulman and T. Venanzi, *J. Am. Chem. Soc.*, **98**, 4701-4705 (1976). Signs for experimental values were chosen on the basis of calculated values and correspond with experimental signs determined in model compounds except as noted. Observed values are for dilute aqueous solutions. [b] Assume molecular geometry of crystalline imidazole at 20 °C as determined from neutron diffraction study of B. M. Craven, R. K. McMullan, J. D. Bell, and H. C. Freeman, *Acta Crystallogr., Sect. B*, **33**, 2585-2589 (1977). [c] Assume molecular geometry of imidazolium ion in crystalline imidazolium dihydrogen orthophosphate as determined by R. H. Blessing and E. L. McGandy, *J. Am. Chem. Soc.*, **98**, 6739 (1976). [d] Assume same imidazole-ring geometry as for imidazole and attach tetrahedral $CH_3$ group at $N_1$ with C-N bond length = 1.47 Å, C-H bond lengths = 1.093 Å, and $C_3$ axis of $CH_3$ group collinear with C-$N_1$ bond. [e] Sign determined from titration curves (Figures 6 and 7). [f] Signs based on assumed correspondence with calculated change on protonation. [g] Assume same ring geometry as for imidazolium ion and attach methyl group at $N_1$ as described in footnote *d*.

**Table III.** Comparison of Experimental $^{13}C^{15}N$ Coupling Constants (Hz) in Various Solvents

| coupling | exptl values $H_2O$ | exptl values $CHCl_3$ | exptl values $CH_2Cl_2$ | calcd values |
|---|---|---|---|---|
| $^1J_{C_2N_1}$ | 12.2 | 11.6 | 11.3 | −11.8 |
| $^1J_{C_2N_3}$ | 1.9 | <1 | <1 | +7.3 |
| $^1J_{C_5N_1}$ | 13.4 | 13.4 | 14.0 | −13.7 |
| $^1J_{C_4N_3}$ | 0.9 | 2.4 | 2.7 | +2.4 |
| $^2J_{C_4N_1}$ | 4.8 | 5.8 | 5.8 | −0.2 |
| $^2J_{C_5N_3}$ | <1 | 1.5 | 1.7 | +2.6 |

**Table IV.** Comparison of 1-Methylimidazole $^{13}C^{15}N$ Couplings (Hz) with Model Compounds

| 1-MeIm (in $CH_2Cl_2$) bond | 1-MeIm (in $CH_2Cl_2$) $J_{CN}$ | pyrrole[b] bond | pyrrole[b] $J_{CN}$ | pyridine[b] bond | pyridine[b] $J_{CN}$ |
|---|---|---|---|---|---|
| $C_2N_1$ | −11.3 | $C_1N$ | −13.0 | | |
| $C_2N_3$ | <±1.0 | | | $C_1N$ | +0.6 |
| $C_5N_1$ | −14.1 | $C_1N$ | −13.0 | | |
| $C_4N_3$ | +2.7 | | | $C_1N$ | +0.6 |
| $C_4N_1$ | (−)5.8[a] | $C_2N$ | −3.9 | | |
| $C_5N_3$ | (+)1.7[a] | | | $C_2N$ | +2.5 |

[a] Signs chosen by comparison with experimental values for pyrrole and pyridine. [b] T. Bundgaard, H. J. Jakobson, and E. J. Rahkamaa, *J. Magn. Reson.*, **19**, 345-356 (1975).

calculated $^{13}C^{15}N$ couplings between nuclei in the imidazole ring are relatively insensitive to the point of attachment of the methyl group.

In spite of the obvious geometrical differences among pyrrole, pyridine, and the imidazoles, surprisingly good agreement is found with comparable $^{13}C^{15}N$ coupling constants, as shown in Table IV. That is especially notable for $J_{C_2N_3}$ in 1-MeIm, where the Blizzard-Santry calculation gives a large positive value, whereas the directly observed value is comparable to that for pyridine. Similarly, the 5.8-Hz $C_4N_1$ coupling in 1-MeIm ($CH_2Cl_2$ solution) corresponds to −3.9 Hz observed for $C_2N$ in pyrrole. Thus, the $^{13}C^{15}N$ couplings seem to support the concept of a "pyrrole-like" ($N_1$) and a "pyridine-like" ($N_3$) nitrogen in imidazole.

Proton-proton coupling constants listed in Table I give best fits to the complex proton-coupled $^{15}N$ and $^1H$ NMR spectra. $^4J_{H_2H_4}$ and $^4J_{H_2H_5}$ for Im are those expected from previous results.[18] $^3J_{H_4H_5}$ and $J_{N_1N_3}$ were observed only in the Im $^{15}N$ spectrum, where they appear as a sum and difference in the submultiplet structure. By comparison with 1-MeIm and $His^-$, $J_{N_1N_3}$ may be taken to be ±1.1 Hz and $^3J_{H_4H_5}$ is then ±1.4 Hz, presumably positive.

**Tautomerism of Histidine in Aqueous Solution.** The data in Table I demonstrate that replacement of hydrogen by a methyl group at $N_1$ has little effect on the couplings between nitrogen and protons in the imidazole ring. Thus, the average of $^2J_{N_1H_2}$ and $^2J_{N_3H_2}$ for 1-methylimidazole gives −9.2 Hz, which represents the average coupling to $H_2$ of a "pyridine-like" nitrogen containing a lone pair of electrons (designated as β-type nitrogen) and a "pyrrole-like" nitrogen (α type) bound to a methyl group. For imidazole a value of −9.6 Hz is observed for the average over a β-type nitrogen and an α-type nitrogen bound to a proton. This suggests that replacement of the methyl group by a proton does not greatly alter the coupling of $N_1$ or $N_3$ to $H_2$. This hypothesis is further supported by noting that the average of $^2J_{N_1H_5}$ and $^2J_{N_3H_4}$ for 1-methylimidazole is nearly the same as the observed average value for

**Table V.** Comparison of Reported Fractions of $\beta N_1$ Tautomer in Aqueous Solutions of Histidine and Several Histidine Derivatives

| NMR parameter used | ref 6 $^{13}C$ shifts | ref 5 $^3J_{C_5H_2}$ | ref 9 $^2J_{N_1H_5}$ | ref 21 $^3J_{C_\beta C_2}$ | our results $^{15}N$ shifts | our results $^2J_{N_1H_5}$ | our results $^1J_{C_5N_1}$ |
|---|---|---|---|---|---|---|---|
| histidine, pH ca. 8 | 0.2 | | 0.12 | 0.24[a] | 0.16 | 0.11 | 0.21 |
| histidine, pH 9.05 | | 0.1 | | | | | |
| histidine, pH >10 | | | 0.2 | 0.5[b] | 0.35 | 0.31 | 0.43 |
| 4-methylimidazole, pH ca. 11 | | 0.4 | | | | | |
| *N*-acetylhistidine, pH ca. 8 | 0.36 | | | | | | |
| glycylhistidylglycine, pH ca. 8 | 0.29 | | | | | | |
| bactitracin, pH ca. 8 | 0.29 | | | | | | |

[a] Based on calculated $^3J_{C_\beta C_2}$ = 5.0 Hz with $NH_4^+$ near $N_3$. [b] Based on calculated $^3J_{C_\beta C_2}$ = 6.2 Hz with $NH_3$ near $N_3$.

**Table VI.** Comparison of Observed $^{13}C^{15}N$ and $^{15}N^1H$ Couplings (Hz) for Imidazole and Histidine Species with Estimates Based on Aqueous 1-Methylimidazole Species

| bond | Im estd | Im obsd | $His^-$ estd | $His^-$ obsd[a] | $His^\pm$ estd | $His^\pm$ obsd[a] | $ImH^+$ estd | $ImH^+$ obsd | $His^{+(2+)}$ estd | $His^{+(2+)}$ obsd[a] |
|---|---|---|---|---|---|---|---|---|---|---|
| $C_2N_1$ | −7.1 | −6.9 | −8.1 | (−6.4)[b] | −10.1 | −10.1 | −16.7 | −16.2 | −16.7 | −16.1 |
| $C_2N_3$ | −7.1 | −6.9 | −6.0 | (−6.9)[b] | −4.0 | −2.7 | −16.7 | −16.2 | −16.7 | −16.0 |
| $C_5N_1$ | −6.3 | −5.9 | −7.7 | −7.3 | −10.5 | −10.4 | −11.4 | −10.6 | −11.4 | −11.6 |
| $C_4N_3$ | −6.3 | −5.9 | −4.8 | −4.7 | −2.0 | (+4.1)[c] | −10.7 | −10.6 | −10.7 | −9.9 |
| $N_1H_2$ | −9.2 | −9.6 | −8.9 | −8.8 | −8.2 | −8.2 | −5.0 | −5.5 | −5.0 | −4.6 |
| $N_3H_2$ | −9.2 | −9.6 | −9.5 | −9.6 | −10.2 | −10.2 | −5.4 | −5.5 | −5.4 | −4.1 |
| $N_1H_5$ | −7.3 | −7.2 | −6.9 | −6.6 | −6.2 | −5.9 | −4.4[d]<br>−5.2 | −4.0[d]<br>−4.6 | −4.4[d]<br>−5.2 | −4.8 |
| $N_3H_5$ | −2.6 | −2.5 | −2.4 | −2.2 | −2.1 | −1.8 | −3.8[d]<br>−4.6 | −4.0[d]<br>−4.6 | −3.8[d]<br>−4.6 | −3.0 |

[a] Data from ref 9. Estimations based on $f_{\beta N_1}$(amphion) = 0.20; $f_{\beta N_1}$(anion) = 0.40. [b] Possible assignment reversal because of data scatter. Both are observed in the $C_2$ multiplet. [c] The observed coupling ±4.1 Hz may be attributable to $^3J_{C_4N_1}$, rather than $^1J_{C_4N_3}$, which is expected to be close to 0, in which case the sign could be either plus or minus. On that basis the estimated value is −3.8 Hz. [d] Analyses of proton spectra yield limits only in these cases.

imidazole. Finally, a comparison of the same couplings in $ImH^+$ and 1-$MeImH^+$ strongly suggests that replacement of the proton by a methyl group at $N_1$ has a comparatively small effect on couplings among imidazole-ring nuclei.

Blomberg et al.[9] have utilized observed N-H couplings in the imidazole ring of histidine to infer relative abundances of the two tautomers of histidine ($\beta N_1$ and $\alpha N_1$) in its amphionic and anionic forms. In their calculation, they assumed that the value of $^2J_{N_1H_5}$ depends only upon whether $N_1$ is protonated ($\alpha N_1$) or deprotonated ($\beta N_1$), taking $^2J_{\alpha N_1H_5} = -4.8$ Hz (their value for $His^+$ where both $N_1$ and $N_3$ are protonated, neglecting any effect of the positive charge on the $N_1H_5$ coupling) and $^2J_{\beta N_1H_5} = -14.4$ Hz, which is an average over literature values for various five-membered heterocyclic ring systems[19,20] containing β-type nitrogen. They then calculated the fraction of $\beta N_1$ tautomer for a given histidine species ($f_{\beta N_1}$) using the expression

$$^2J_{N_1H_5}(\text{obsd}) = -14.4f_{\beta N_1} - 4.8(1 - f_{\beta N_1})$$

From their observed $^2J_{N_1H_5}$ values for the amphionic and anionic forms of histidine (−5.9 and −6.6 Hz, respectively) they calculated $f_{\beta N_1}$ = 0.12 at pH 8.2 and 0.2 at pH >9.3, where the anion predominates.

We may check those calculated values of $f_{\beta N_1}$ for the amphionic and anionic forms of histidine using the $^{15}N$ shift data for Im and 1-MeIm as a function of pH. The data strongly support the conclusion that deprotonation of a given nitrogen in the imidazole ring produces a +73-ppm shift at that nitrogen and a −8.0-ppm shift at the other nitrogen, whether the other nitrogen is bound to a methyl group or a proton. Thus, if deprotonation of the cationic form of histidine to form the amphion requires deprotonation at $N_1$ to form the $\beta N_1$ tautomer and deprotonation at $N_3$ to form the $\alpha N_1$ tautomer, then the observed shift of $^{15}N_1$ between the cationic and amphionic forms is given by

$$\Delta_{N_1}{}^{-H} = +73.0f_{\beta N_1} - 8.0(1 - f_{\beta N_1})$$

assuming, of course, that the $^{15}N$ shifts for the imidazole nitrogens of histidine are the same as those for Im or 1-MeIm. Neglecting any direct effects of deprotonation of the primary amine group, the same equation can be used to calculate $f_{\beta N_1}$ for the anion where $\Delta_{N_1}{}^{-H}$ is the observed $^{15}N_1$ shift change between the cationic and anionic forms of histidine. Using the $\Delta_{N_1}{}^{-H}$ values of Blomberg et al.[9] (+5.0 ppm for the amphion and +20.7 ppm for the anion) we calculate $f_{\beta N_1}$ = 0.16 and 0.35 for the amphion and anion, respectively. The difference between these $f_{\beta N_1}$ values and those calculated by Blomberg et al.[9] is attributable primarily to their choice of $^2J_{\beta N_1H_5} = -14.4$ Hz for the $\beta N_1$ tautomer. Based upon our previously noted correlations between the measured coupling constants for Im and 1-MeIm in Table I, we believe that a much more reliable estimate of $^2J_{\beta N_1H_5}$ is given by $^2J_{N_3H_4}$ in 1-MeIm, viz., −9.0 Hz. Similarly, we would set $^2J_{\alpha N_1H_5} = {}^2J_{N_1H_5}$(1-MeIm) = −5.5 Hz. Then, for a given histidine species

$$^2J_{N_1H_5}(\text{obsd}) = -9.0f_{\beta N_1} - 5.5(1 - f_{\beta N_1})$$

Using the observed $^2J_{N_1H_5}$ values of Blomberg et al.[9] we obtain $f_{\beta N_1}$ = 0.11 for the amphion and 0.31 for the anion. A comparable calculation based on $J_{C_5N_1}$, in which $J_{C_5\beta N_1} = J_{C_4N_3}$(1-MeIm) = +0.9 Hz and $J_{C_5\alpha N_1} = J_{C_5N_1}$(1-MeIm) = −13.4 Hz, yields $f_{\beta N_1}$ = 0.21 for the amphion and 0.43 for the anion. A comparison of the various values reported in the literature and the bases for their estimation are given in Table V. The scatter in those results led us to consider all of the CN and NH coupling constants available from this work and the histidine values of Blomberg et al.[9] With the assumption that $f_{\beta N_1}$ = 0.20 in $His^\pm$ and 0.40 in $His^-$ the estimated values were obtained to compare with observations in Table VI. A similar comparison for Im, on the basis of equal tautomer abundances, is also given there. Estimated $ImH^+$ and $His^+$ constants are those observed for 1-$MeImH^+$.

The assumed tautomer abundances in $His^-$ are essentially the same as those derived for 4-MeIm[5] and N-blocked histidine

derivatives.[6] This strongly suggests that stabilization of the $\alpha N_1$ tautomer in $His^-$ does not result from hydrogen bonding between the primary amine protons and $\beta N_3$ of the imidazole ring but rather may be largely attributable to electronic or steric consequences of substitution at $C_4$. In $His^{\pm}$, on the other hand, the decreased stabilization of the $\beta N_1$ tautomer may be indicative of significant hydrogen bonding between the primary aminium protons and $\beta N_3$ of the imidazole ring. In view of the greater overall consistency of all the results, it seems to us that $J_{C_5N_1}$ may be the parameter best suited for estimation of tautomeric abundances in these systems.

## Conclusions

It is perhaps surprising that ring coupling constants in the imidazole derivatives are so closely similar to those in imidazole itself. However, as the calculated values reflect similar behavior, and correspondence with observed coupling constants for equivalent bonds in such divergent structures as pyrrole and pyridine is quite good (Table IV), it must be concluded that they are not really sensitive indicators of structural features other than protonation or deprotonation of the pyridine-like nitrogen ($N_3$). While it is tempting to rely more heavily on $^{15}N$ chemical shifts or NH couplings as indicators for such protonation or deprotonation, it should be noted that for NH couplings the range of values between protonation extremes is relatively small and for $^{15}N$ shifts effects of the extramolecular environment can be large.[10,11] It therefore seems that $^1J_{CN}$ may the NMR parameter best suited for estimating the degree of protonation of imidazole-ring $N_3$ under the most general conditions.

The largest discrepancies noted in this work are between the observed and calculated values for $J_{C_4N_1}$ and $J_{C_2N_3}$ in 1-methylimidazole. As the observed values do not appear to be solvent dependent to any appreciable extent and the calculated values do not change significantly upon incorporation of hydrogen-bonded structures, we are unable to suggest a resolution for the discrepancies.

**Acknowledgment.** This work was performed under the auspices of the U.S. Department of Energy.

## References and Notes

(1) (a) The Los Alamos Scientific Laboratory. (b) The University of Texas.
(2) (a) Sundberg, R. J.; Martin, R. B. *Chem. Rev.* **1974**, *74*, 471 (cf. p 495). (b) Bachovchin, W. W.; Roberts, J. D. *J. Am. Chem. Soc.* **1978**, *100*, 8041.
(3) Alei, M., Jr.; Morgan, L. O.; Wageman, W. E. *Inorg. Chem.* **1978**, *17*, 2288, 3314.
(4) Wasylishen, R. E.; Tomlinson, G. *Biochem. J.* **1975**, *147*, 605.
(5) Wasylishen, R. E.; Tomlinson, G. *Can. J. Biochem.* **1977**, *55*, 579.
(6) Reynolds, W. F.; Peat, I. R.; Freedman, M. H.; Lyerla, J. R., Jr. *J. Am. Chem. Soc.* **1973**, *95*, 328.
(7) Reynolds, W. F.; Freedman, M. H. *J. Am. Chem. Soc.* **1974**, *96*, 570.
(8) Kawano, K.; Kyogoku, Y. *Chem. Lett.* **1975**, 1305.
(9) Blomberg, F.; Maurer, W.; Rüterjans, H. *J. Am. Chem. Soc.* **1977**, *99*, 8149.
(10) Alei, M. Jr.; Wageman, W. E. *Tetrahedron Lett.* **1979**, 667-670.
(11) Schuster, I. I.; Roberts, J. D. *J. Org. Chem.* **1979**, *44*, 3864.
(12) Nicolet Instrument Corp., NIC-05-40417, revised Sept 1972.
(13) Pople, J. A.; Schneider, W. G.; Bernstein, H. J. "High Resolution Nuclear Magnetic Resonance", McGraw-Hill, New York, 1959.
(14) Becker, E. D. "High Resolution NMR", Academic Press, New York, 1969.
(15) Alei, M. Jr.; Florin, A. E. *J. Phys. Chem.* **1968**, *72*, 550.
(16) Schulman, J. M.; Venanzi, T. *J. Am. Chem. Soc.* **1976**, *98*, 4701, 6739.
(17) Blizzard, A. C.; Santry, D. P. *J. Chem. Phys.* **1971**, *55*, 950.
(18) Wang, S. M.; Li, N. C. *J. Am. Chem. Soc.* **1966**, *88*, 4592.
(19) Lichter, R. L.; Roberts, J. D. *J. Am. Chem. Soc.* **1971**, *93*, 5218.
(20) Kintzinger, J. P.; Lehn, J. M. *Chem. Commun.* **1967**, 660. *Mol. Phys.* **1968**, *14*, 133.
(21) London, R. E. *J. Chem. Soc., Chem. Commun.* **1978**, 1070.

# Electronic Spectra and Structure of a Weak $\pi$ Complex. Vibronic Structure in the Charge-Transfer Transition of Anthracene–*s*-Trinitrobenzene

**C. J. Eckhardt†* and H. Eckhardt**

*Contribution from the Department of Chemistry, University of Nebraska, Lincoln, Nebraska 68588.* *Received August 20, 1979*

**Abstract:** Polarized specular reflection and absorption spectra for the crystalline anthracene-*s*-trinitrobenzene complex are reported at 20 and 5 K. The quantitative assignment of the polarization of the CT transition of the asymmetric complex places the moment near the line-of-centers. An irregular vibrational progression of ~1400 $cm^{-1}$ is observed for the CT transition. A second CT band is observed at 31 000 $cm^{-1}$. The first and second singlet transitions of anthracene are observed and are found to have free molecule frequencies, intensities, and polarizations. A band seen at 44 000 $cm^{-1}$ is interpreted as a trinitrobenzene molecular transition. The use of crystals of complexes for study of *molecular* spectra is suggested.

## I. Introduction

Recent work in our laboratory has been concerned with the electronic spectra and structure of electron donor-acceptor (EDA) complexes in crystals.[1-3] In an effort to further understand the nature of this interaction, we have been particularly concerned with the effects of varied acceptors with a specific donor molecule, namely, anthracene. Previous studies of anthracene crystalline complexes with TCNQ[0,1] and pyromelletic dianhydride[2,4] have been made with detailed examination of the excitonic interactions of the latter reported by other workers.[5,6] The concern in our investigations has been centered, insofar as possible, upon the molecular manifestation of the EDA interaction.

The complex of 1,3,5-trinitrobenzene (TNB) with anthracene (A) is one which has been extensively studied. Early work on the complex was done in solution and in organic glasses.[7-9] Later work on crystalline films of TNB-A[10,11] was reported but, since such a study for a single crystal orientation cannot absolutely assign the charge-transfer (CT) transition moment in this asymmetric complex, further study is necessary to obtain the assignment. Below is shown the projection of TNB onto the plane of A.

† John Simon Guggenheim Fellow, 1979-1980.

0002-7863/80/1502-2887$01.00/0 